Biotechnology Notes 3 (2022) 15–24

Contents lists available at ScienceDirect

Biotechnology Notes

journal homepage: www.keaipublishing.com/en/journals/biotechnology-notes/

Model-based dynamic engineering of *Escherichia coli* for N-acetylglucosamine overproduction

Jiangong Lu [a,b,1], Yaokang Wu [a,b,1], Chen Deng [a,b], Yanfeng Liu [a,b], Xueqin Lv [a,b], Jianghua Li [a,b,**], Guocheng Du [a,b], Long Liu [a,b,*]

[a] Key Laboratory of Carbohydrate Chemistry and Biotechnology, Ministry of Education, Jiangnan University, Wuxi, 214122, China
[b] Science Center for Future Foods, Jiangnan University, Wuxi, 214122, China

ARTICLE INFO

Keywords:
N-Acetylglucosamine
Escherichia coli
Metabolic engineering
etabolic network model
Dynamic regulation

ABSTRACT

N-acetylglucosamine (GlcNAc), a glucosamine derivative, has a wide range of applications in pharmaceutical fields, and there is an increasing interest in the efficient production of GlcNAc genetic engineered bacteria. In this work, *Escherichia coli* ATCC 25947 (DE3) strain was engineered by a model-based dynamic regulation strategy achieving GlcNAc overproduction. First, the GlcNAc synthetic pathway was introduced into *E. coli*, and through flux balance analysis of the genome-scale metabolic network model, metabolic engineering strategies were generated to further increase GlcNAc yield. Knock-out of genes *poxB* and *ldhA,* encoding pyruvate oxidase and lactate dehydrogenase, increased GlcNAc titer by 5.1%. Furthermore, knocking out N-acetylmuramic acid 6-phosphate etherase encoded by *murQ* and enhancing glutamine synthetase encoded by *glnA* gene further increased GlcNAc titer to 130.8 g/L. Analysis of metabolic flux balance showed that GlcNAc production maximization requires the strict dynamic restriction of the reactions catalyzed by *pfkA* and *zwf* to balance cell growth and product synthesis. Hence, a dynamic regulatory system was constructed by combining the CRISPRi (clustered regularly interspaced short palindromic repeats interference) system with the lactose operon *lacI* and the transcription factor pdhR, allowing the cell to respond to the concentration of pyruvate and IPTG to dynamically repress *pfkA* and *zwf* transcription. Finally, the engineered bacteria with the dynamic regulatory system produced 143.8 g/L GlcNAc in a 30-L bioreactor in 55 h with a yield reaching 0.539 g/g glucose. Taken together, this work significantly enhanced the GlcNAc production of *E. coli.* Moreover, it provides a systematic, effective, and universal way to improve the synthetic ability of other engineered strains.

1. Introduction

D-glucosamine (GlcN) and its acetylated derivative N-acetylglucosamine (GlcNAc) are found in various species, including microorganisms, plants, and animals.[1] GlcNAc is the basic unit of some important polysaccharides in human cells and is widely applied in health care products and cosmetics.[2,3] It is also extensively used for medicines due to its excellent effect on articular cartilage regeneration.[1]

At present, there are three main ways to produce GlcNAc, chitin hydrolysis, biotransformation, and microbial synthesis. Microbial synthesis has a high yield and high efficiency and has a lower environmental impact than the other two methods.[4] At present, the highest reported GlcNAc titer in *Corynebacterium glutamicum* was 117.1 g/L in a 50-L bioreactor in 75 h,[5] and 131.6 g/L in *Bacillus subtilis* in a 15-L bioreactor in 77 h.[6] As host bacteria, *E. coli* has many advantages, including clear genetic background, perfect expression system, easy gene-editing, rapid growth, cost-saving, and strong anti-pollution ability. In previous studies, the knockout of *manXYZ* and *nagABE* genes blocked glucosamine transport and consumption in *E. coli*.[7] Then, a GlcNAc titer exceeding 110 g/L in 1-L bioreactors was achieved by overexpressing two key genes, *glmS* (encoding GlcN-6-phosphate synthase) and *GNA1* (encoding GlcNAc-6-phosphate N-acetyltransferase).[7] Ma et al. balanced cell growth and GlcNAc synthesis using glycerol and glucose as mixed carbon sources for *E. coli*, and the GlcNAc titer was further increased to 179.7 g/L.[8] However, there are still many acidic metabolic pathways by-products in this strain, such as acetate and

* Corresponding author. Key Laboratory of Carbohydrate Chemistry and Biotechnology, Ministry of Education, Jiangnan University, Wuxi 214122, China.
** Corresponding author. Key Laboratory of Carbohydrate Chemistry and Biotechnology, Ministry of Education, Jiangnan University, Wuxi 214122, China.
E-mail addresses: lijianghua@jiangnan.edu.cn (J. Li), longliu@jiangnan.edu.cn (L. Liu).
[1] These authors contributed equally to this work.

https://doi.org/10.1016/j.biotno.2022.02.001
Received 24 December 2021; Received in revised form 25 January 2022; Accepted 3 February 2022
Available online 5 February 2022

lactate. This can result in carbons loss, reduced economy, and limited productivity in the production process. Acetate and other by-products can also inhibit cells growth.[9]

The genome-scale metabolic network model (GSMM) contains most of the biochemical reactions of specific microorganisms. Through GSMM, the correlation and dependence between different metabolic reactions can be identified, and targeted regulation strategies can be guided genome-wide perspective.[10] There are many mature and reliable algorithms such as FBA (Flux Balance Analysis), OptKnock, and Minimization Of Metabolic Adjustment (MOMA) to formulate metabolic engineering strategies and simulate the metabolic reactions flux of cells. For example, it was reported that knockout and overexpression targets predicted separately using the OptForce algorithm based on GSMM iAF1260 increased intracellular propionyl-CoA levels by 4-fold in *E. coli BL21*.[11] At present, GSMM of *E. Coli* is developing rapidly and has been widely used for metabolic engineering.

This work engineered a GlcNAc producing strain by introducing the synthetic pathway and blocking the catabolism pathway (Fig. 1). Then a GSMM iML1515_GlcNAc was built by adding GlcNAc synthesis reactions into the *E. coli* GSMM iML1515,[12] and used to analyze metabolic pathways. According to the model simulation results, various metabolic engineering strategies were performed to improve GlcNAc production. First, the *poxB* and *ldhA* knockout reduced the production of by-products acetate and lactate. Second, the enhancement of *glnA* and the knockout of *murQ* further increased the accumulation of GlcNAc. Third, the *pfkA* and *zwf* genes were interfered dynamically by the CRISPRi (clustered regularly interspaced short palindromic repeats interference) system combined with the transcription factor PdhR. The GlcNAc titer exceeded 140 g/L in 55 h in a 30-L bioreactor, and the yield reached 0.539 g/g glucose. In addition, the model-guided metabolic engineering strategies proposed here may be used to construct other microbial cell factories.

2. Materials and methods

2.1. Bacterial strains and plasmids

All strains and plasmids used in this study are listed in Table 1. The primers used in this study are listed in Table S1. All microorganisms were grown at 37 °C in Luria–Bertani (10 g/L tryptone, 5 g/L yeast extract, 10 g/L NaCl) broth or LB agar plates.

2.2. DNA manipulation and construction of plasmids

The *GNA1* gene from *S. cerevisiae S288C* and *glmS* gene from *E. coli ATCC 25947 (DE3)* were respectively connected to the pET28a plasmid by seamless cloning, resulting in pET28a-*GNA1* and pET28a-*glmS*. Then the cassettes templates of P_{T7lac}-*GNA1* and P_{T7lac}-*glmS** were obtained by polymerase chain reaction (PCR). The *glmS*54* screened by Deng et al. contains a triple mutation (A38T, R249C, G471S) that effectively reduces the inhibitory effect of the product.[13] PCR was performed on pET28a-*glmS* by designing primers to make a single base mutation. Then, the linear PCR product was transformed into *E. coli JM109* for circularization and cultured on a solid LB medium plate. Recombinant plasmids with related genes were verified by PCR and confirmed by DNA sequencing. After the plasmid with the correct mutation was selected, the above process was repeated for the next mutation step, until pET28a-*glmS*54* was obtained.

The CRISPRi system, used for the dynamic regulation of related pathways, was expressed on plasmid pACYC-duet1. This system contains a *dCas9* and a sgRNA. The *dCas9* gene under the lacUV5 promoter and the sgRNA gene under the P_{J23119} promoter were connected to the vector by a seamless cloning kit. In addition, the *lacO* sequence and the *pdhR* binding site were designed in the primers and added upstream of the *dCas9* gene by PCR to form the P_{lacUV5}-*lacO-pdhR-dCas9* expression cassette. Each target's 20 bp spacer sequence was designed through the CHOPCHOP website (chopchop.cbu.uib.no). After the target sequence primers were designed, the plasmid was amplified by PCR into linear DNA and transformed into *E. coli JM109* for circularization and the plasmid was extracted for Sanger sequencing.

2.3. Gene knockout and integration

Knockout of *poxB*, *ldhA*, *pta*, *ackA*, *yccX,* and *murQ* genes and integration of *GNA1*, *glmS*, *yqaB*, *aceE,* and *glnA* genes were achieved

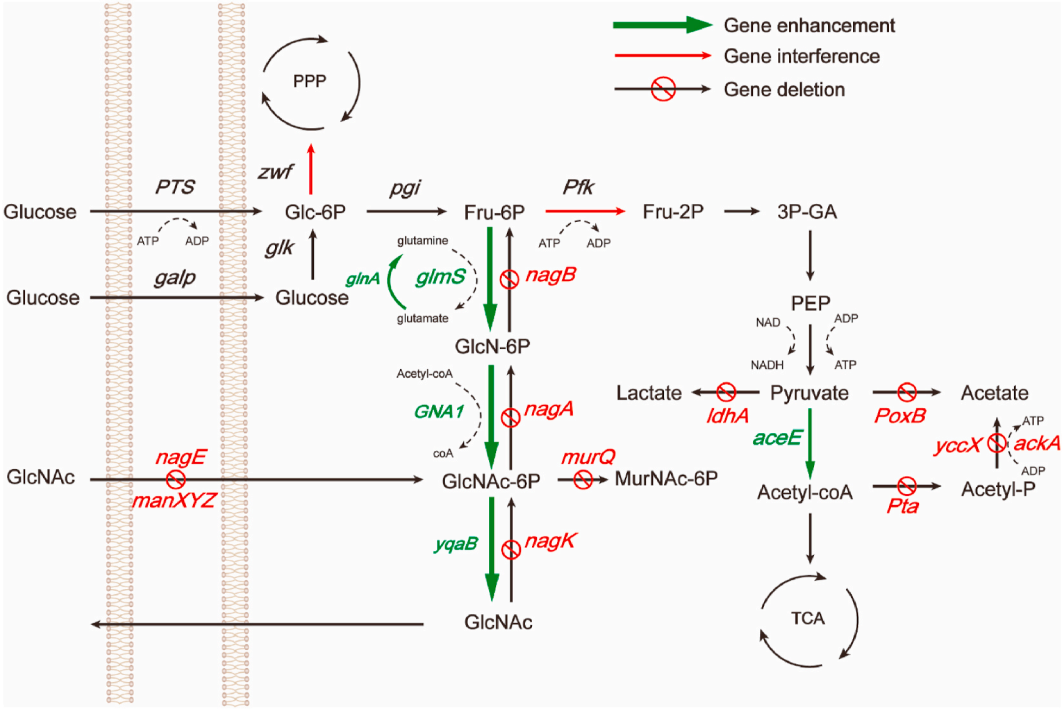

Fig. 1. The metabolic pathway of N-acetylglucosamine (GlcNAc) synthesis in *Escherichia coli*.

Table 1
Strains and plasmids used in this work.

Name	Description	Source
E. coli ATCC 25947 (DE3)	starting strain	Lab stock
E. coli JM109	cloning host	Lab stock
E. coli DH5α	cloning host	Lab stock
G-0	*E. coli ATCC 25947 (DE3)* Δ*manXYZ*:: P_{T7}-*GNA1* Δ*nagABE*:: P_{T7}-*glmS*	This work
G-1	*E. coli ATCC 25947 (DE3)* Δ*manXYZ*:: P_{T7}-*GNA1* Δ*nagABE*:: P_{T7}-*glmS**	This work
G-2	*E. coli ATCC 25947 (DE3)* Δ*manXYZ*:: P_{T7lac}-*GNA1* Δ*nagABE*:: P_{T7lac}-*glmS**	This work
G-3	G-2, Δ*FucIK*::P_{T7lac}-*GNA1*	This work
G-4	G-2, Δ*FucIK*::P_{T7lac}-*glmS**	This work
G-5	G-2, Δ*FucIK*::P_{T7lac}-*glmS**- P_{T7lac} -*GNA1*	This work
G-7	G-3, Δ*poxB* Δ*LdhA*	This work
G-8	G-7, Δ*pta*	This work
G-9	G-7, Δ*ackA*	This work
G-10	G-7, Δ*yccX*	This work
G-11	G-7, Δ*nagK*	This work
G-12	G-7, Δ*murQ*	This work
G-13	G-7, Δ*LdhA*::P_{T7lac}-*yqaB*	This work
G-14	G-7, Δ*LdhA*::P_{T7lac}-*aceE*	This work
G-15	G-7, Δ*LdhA*::P_{T7lac}-*glnA*	This work
G-16	G-15, Δ*murQ*	This work
G-17	G-16-pACYC-P_{lacUV5}-*pdhR* box-*lacO*-*dCas9*-P_{J23119}-sgRNA1-*pfkA2*-sgRNA2-*zwf1*	This work
pKD4	Amp^R, Cm^R, FRT-Cm^R-FRT template	Lab stock
pKD46	Amp^R, λ-red recombinase expression vector	Lab stock
pCP20	Amp^R, Cm^R, *FLP* expression vector	Lab stock
pET-28a	Kan^R, Expression vector	Lab stock
pACYCDuet1	Cm^R, Expression vector	Lab stock
ptargetF[33]	Spc^R, PJ23119-sgRNA	Lab stock
pET28a-*sfGFP*	Kan^R, Fluorescent reporter gene *sf-GFP* expression vector under the control of *lacI* and *pdhR*	This work
pACYC-*dCas9*-sgRNA	Cm^R, Expression vector of sgRNA and *dCas9*	This work
pACYC-*pdhR* box-*lacO*-*dCas9*-P_{J23119}-sgRNA	Cm^R, Expression vector of sgRNA and *dCas9* under the control of *lacI* and *pdhR*	This work
pACYC-*pdhR* box-*lacO*-*dCas9*-P_{J23119}-sgRNA1-sgRNA2	Cm^R, Expression vector of 2 sgRNA and *dCas9* under the control of *lacI* and *pdhR*	This work

through λ-Red homologous recombination.[14] The homologous recombination fragments required for knockout and integration must first be constructed. Gene knockout requires three DNA fragments to be ligated, including the upstream homology arm, the downstream homology arm, and the resistance gene with FRT sites on both ends. At this time, since there are fewer fragments, overlapping extension PCR was used to achieve efficient ligation. A suitable overlap area was designed according to the annealing temperature of the area where the segments need to be connected. After all the fragments were obtained, further fusion amplification was performed to obtain the required recombinant fragments. Four or more fragments are required for ligation when integrating genes into the genome. However, in overlapping extension, PCR is difficult to guarantee efficiency and accuracy; therefore, the seamless cloning kit is used to ligate multiple fragments into one vector. Then PCR was used to amplify the required recombinant fragments. In this study, the 800–1000 bp homology arm can achieve effective recombination efficiency regardless of knockout or integration.

To induce the λ-Red homologous recombination system expression, the strain with pKD46 was cultured in LB medium with 50 mmol/L arabinoses for more than 1 h at 30 °C until the OD_{600} reached 0.6. Then the cells were transformed into competent cells by chemical or electroporation methods. After that, the previously constructed homologous recombination fragments were transformed into competent cells. The successfully knocked out or integrated strains were selected by colony PCR, and the pCP20 plasmid was transformed into these strains to eliminate the antibiotic resistance gene flanked by FRT sites. The strains were cultured in an antibiotic-free LB medium at 37 °C and 42 °C overnight to eliminate the temperature-sensitive plasmids pKD46 and pCP20.

2.4. Shake flask fermentation

The shake flask fermentation medium contains 10 g/L glucose, 4.8 g/L yeast extract, 2.4 g/L tryptone, 1 g/L glycerin, 11.2 g/L KH_2PO_4, 8 g/L K_2HPO_4, 4 g/L citric acid monohydrate, 3.36 g/L $MgSO_4{\cdot}7H_2O$ 10 g/L $(NH_4)_2SO_4$, 0.02 g/L $CaCl_2$, 6 g/L urea, and 1 mL/L mixture of trace elements. Concentrated ammonia water was added to adjust the pH to 7.0 before sterilization. The trace element mixture includes 0.1 g/L $CoCl_2{\cdot}6H_2O$, 0.1 g/L CuSO4·$5H_2O$, 5 g/L $FeSO_4{\cdot}7H_2O$, 0.33 g/L $MnSO_4{\cdot}H_2O$, and 3.8 g/L $ZnSO_4{\cdot}7H_2O$.

A single colony grown on the solid LB medium was picked and inoculated into a shake flask with baffle containing liquid LB medium for cultivation for 10–12 h at 37 °C and 220 rpm as a seed for fermentation. The cultivated seeds were added to a 500 mL baffled shake flask with 50 mL of fermentation medium at a 10% inoculum ratio. Fermentation was performed at 37 °C and 220 rpm for 65 h 1g calcium carbonate powder was added to each shake flask as a pH stabilizer to avoid the rapid decrease in pH caused by acidic metabolites produced during fermentation. The pH of the fermentation broth was tested every 6 h and adjusted to about 7.0 with ammonia water. While adjusting the pH, the fermentation broth was sampled to detect glucose concentration. The inducer IPTG was added at the 6th hour of fermentation to turn on the expression of key genes. When the glucose concentration in the fermentation broth was lower than 1 g/L, 500 g/L glucose was added to the fermentation broth to improve glucose concentration to 20 g/L. Maintaining glucose concentration below 20 g/L and replenishing it nearly depletion prevented the glucose effect that inhibits the transport of inducer IPTG into the cell.

2.5. Fed-batch fermentation in a 30-L bioreactor

The seed medium contained 10 g/L glucose, 3 g/L yeast extract, 1 g/L glycerin, 8 g/L KH_2PO_4, 10 g/L K_2HPO_4, 1 g/L citric acid monohydrate, 0.5 g/L $MgSO_4{\cdot}7H_2O$, 5 g/L $(NH_4)_2SO_4$, 0.02 g/L $CaCl_2$, and 1 mL/L mixture of trace elements. The pH was adjusted to 7.0 by adding ammonia. Colonies grown on the plates overnight were cultured in liquid LB medium for 10–12 h at 37 °C and 220 rpm. Then, the cultures were transferred to a baffled shake flask containing fresh seed culture medium and incubated at 37 °C for 10–12 h at 220 rpm according to the 3% inoculum volume.

The 30-L bioreactor fermentation medium contained 5 g/L glucose, 4.8 g/L yeast extract, 2.4 g/L tryptone, 1 g/L glycerin, 6.67 g/L KH_2PO_4, 2.8 g/L K_2HPO_4, 3.5 g/L citric acid monohydrate, 2.48 g/L $MgSO_4{\cdot}7H_2O$, 4 g/L $(NH_4)_2SO_4$, 0.02 g/L $CaCl_2$, 6 g/L urea, and 1 mL/L mixture of trace elements. The seeds were added to the bioreactor at a

10% inoculation rate, and the total volume after inoculation was 15 L. The pH was automatically adjusted by adding ammonia water, and it was always maintained at about 7.0 during the fermentation process. The dissolved oxygen was maintained at 30%–50% by adjusting the ventilation volume, stirring speed, and glucose feeding speed. The fermentation process lasted 55–65 h at 37 °C. Fed-batch cultivation was performed with an initial glucose concentration of 5.0 g/L. When glucose was depleted, 5000–7000 mL of concentrated glucose (800 g/L) was added to the medium.

2.6. Metabolic network model of Escherichia coli

The genome-wide metabolic network model of *E. coli* iML1515 was obtained from the BiGG database (bigg.uscd.edu). The acetylation reaction of Glc-6P catalyzed by *GNA1,* the dephosphorylation reaction of GlcNAc-6P, and the transport reaction of GlcNAc were added to the model, and other GlcNAc synthesis reactions were already included in iML1515. CobraToolbox 2.0 was obtained from the GitHub website (github.com).[15]

2.7. Analytic methods

The fluorescence of super fold green fluorescent proteins (sf-GFP) was detected by a Cytation microplate reader (BioTek) (excitation, 480 nm; emission, 516 nm). GlcNAc, lactate, acetate, and gluconate concentrations in the fermentation broth were measured via high-performance liquid chromatography using an HPX-87H column (Bio-Rad Hercules, CA, USA) and a refractive index detector. Sulfuric acid with a concentration of 5 mmol/L was used as the mobile phase with a flow rate of 0.6 mL/min at 35 °C. The glucose and glutamate concentrations in the supernatant were measured using a glucose-glutamate analyzer (SBA-40C; Biology Institute of Shandong Academy of Sciences, Jinan, China).

2.8. Statistical analysis

Three independent replicates were performed for all experiments. Differences between two groups were determined by two-tailed Student's t-test and one-way ANOVA followed by post-hoc Dunnett's test for multiple groups. *P < 0.05 and **P < 0.01.

3. Results

3.1. Construction of GlcNAc producing strains

E. coli ATCC 25947 (DE3) was used as the starting strain to produce GlcNAc. First, a heterogenous GlcNAc-6-phosphate N-acetyltransferase gene was introduced into the starting strain. For this purpose, the *GNA1* encoding GlcNAc-6-phosphate N-acetyltransferase of *S. cerevisiae* with efficient catalytic activity in *E. coli*[7] was selected. In addition, the feedback inhibition of GlcN-6-phosphate synthase *glmS* by GlcN-6P needs to be rescued. *glmS* mutant (*glmS*54*), which reduces the GlcN-6P inhibition, was obtained by error-prone PCR in *E. coli* by Deng et al.[13] Therefore, *glmS*54* was used to strengthen GlcNAc synthesis. P_{T7}-*GNA1* and P_{T7}-*glmS** cassettes were both integrated into the genome of the engineered *E. coli* strain. Moreover, to block GlcNAc absorption and utilization by the strain to increase product accumulation, *manXYZ* and *nagABE* genes related to GlcNAc utilization were knocked out, resulting in the G-1 strain.

Although the G-1 strain showed growth inhibition, it can synthesize 22.6 g/L GlcNAc after 65 h of IPTG-induced shake flask fermentation (Fig. 2A). Furthermore, 17.7 g/L GlcNAc was produced without IPTG addition. These results suggest that the leaked expression of T7 RNA polymerase leads to efficient transcription of genes under the control of the T7 promoter, and severe leaked expression may cause cell growth inhibition. Therefore, the T7 promoter in G-1 was replaced with the T7lac promoter, resulting in strain G-2. The *lacO/lacI* system showed an effective inhibitory effect in G-2. Only less than 1 g/L of GlcNAc was detected in the shake flask fermentation broth without IPTG. Moreover, there is no apparent difference between the growth of the G-2 and the starting strains. The IPTG-induced GlcNAc production in the shake flask reached 25.4 g/L (Fig. 2A). Subsequently, strains were constructed with different copy numbers of the *GNA1* and *glmS* genes, generating strains G-3, G-4, and G-5. As shown in Fig. 2A, GlcNAc was not detected in the fermentation broth of the starting strain, and the most productive strain was G-3, which has two copies of P_{T7lac}-*GNA1* and one copy of P_{T7lac}-*glmS** and can synthesize 30.7 g/L GlcNAc in a shake flask. Fed-batch fermentation of strain G-3 in a 30-L bioreactor, yields GlcNAc titers and a cell density of 118.9 g/L and 98.5 (OD_{600}) (Fig. 2C). The GlcNAc titer of the G-3 strain in the bioreactor was 25.1% higher than the G-1 strain (Fig. 2B).

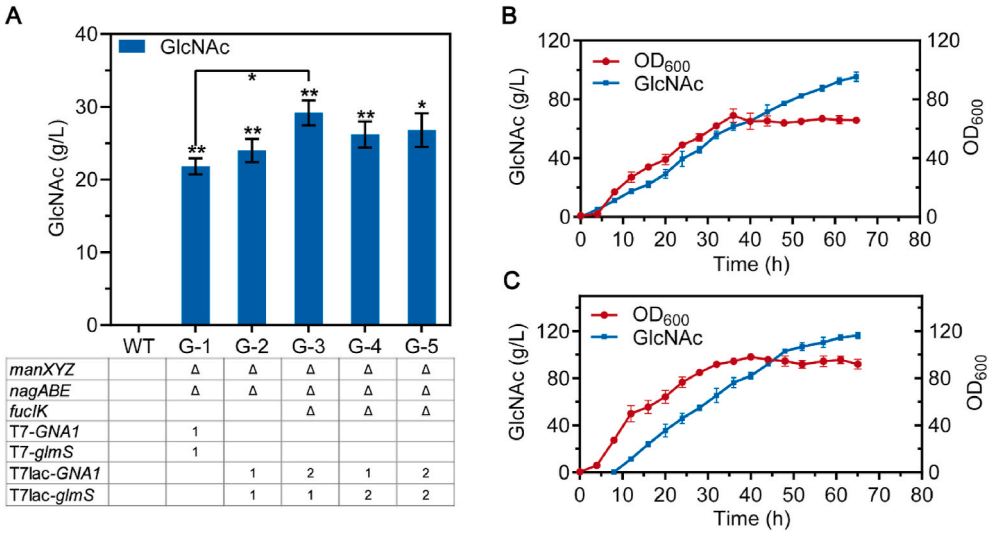

Fig. 2. *glmS* and *GNA1* copy number optimization. (A) Shake flask fermentation results of strains with different copy numbers. Δ means knockout; the number means copy number. (B) Fermentation results of strain G-1 in a 30-L bioreactor. (C) Fermentation results of strain G-3 in a 30-L bioreactor. ** and * symbols indicate p < 0.01 and 0.01 <p < 0.05 relative to the control strain, respectively, except for pairwise comparisons indicated in the figure.

3.2. Model simulation of GlcNAc synthesis

To perform model simulation of GlcNAc synthesis, all GlcNAc synthesis reactions were added to the *E. coli* GSMM iML1515, resulting in iML1514-GlcNAc (Fig. 3A). First, the relationship between growth rate, glucose consumption rate, and GlcNAc synthesis rate was analyzed through the model. The changes of GlcNAc synthesis rate were obtained for different growth rates and glucose consumption rates by targeting the GlcNAc synthesis reaction under various nutrients and sufficient oxygen conditions. The results show that the GlcNAc synthesis rate decreases with the growth rate increase (Fig. 3B). In optimized CbModel function calculation, the growth rate was zero at the theoretical maximum synthesis rate. Second, the growth data of this strain in the 30-L bioreactor was input into the model, and the growth curve was fitted by interpolation. The specific growth rate was set as the constraint condition of the model, which, combined with the approximate actual glucose consumption, was used to calculate the optimal synthesis rate of GlcNAc at each moment. The resulting rate was multiplied by the cell dry weight at the corresponding time, and then multiplied by differential time, the titer increment at different times was obtained. Finally, these increments were summed and the total titers were obtained. The ideal titer of GlcNAc should be between 150 g/L - 160 g/L. The difference between the simulation and the actual titer was 27%.

The Flux Variability Analysis (FVA) was mainly used to investigate the range of flux changes in each reaction under the most ideal situation.[16] The simulation condition was set as 10 mmol·gDW^{-1}h^{-1} glucose absorption rate and the lower limit of the specific growth rate as 0.1. Assuming that other nutrients were sufficient, two sets of metabolic flow data were obtained, the maximum and minimum. By comparison, 217 reactions are not zero in the maximum and minimum metabolic fluxes. Reactions with flux less than 0.0001 mmol·gDW^{-1}h^{-1} have defaulted to 0. The genes that catalyze these reactions were considered non-knockout in the GlcNAc synthesis. Knockout may result in decreased yield or too low a specific growth rate. The flux of POX (*poxB*) and LDH_D (*ldhA*) reactions producing acetate and lactate was 0. The two reactions were set to different fluxes and simulated again. The results show that the biomass growth rate and the GlcNAc synthesis rate decrease with the upregulation of POX and LDH_D (Fig. 3C).

3.3. Blocking of competition pathway and enhancement of GlcNAc synthesis pathway

In G-3, there were high concentrations of acetate and lactate in the fermentation broth, especially when glucose concentration reached 20 g/L. Acetate concentration reached 13.4 g/L, and lactate concentration reached 7 g/L. Lactate and acetate accumulation was toxic for cell growth and competed with GlcNAc synthesis for carbon sources.[9] In *E. coli*, *poxB* catalyzes the oxidation of pyruvate to acetate and carbon dioxide, and *ldhA* catalyzes the production of D-lactate from pyruvate.[17] In addition, based on the simulation results, the above two reactions inhibit biomass growth and inhibit the synthesis of GlcNAc. Thus, Red homologous recombination further knocked out *poxB* and *ldhA* genes resulting in strain G-7. In shake flask fermentation, the acetate concentration decreased to 6 g/L, and the GlcNAc titer reached 33.2 g/L. Moreover, lactate was not detected in the fermentation broth. G-7 strain fermentation experiments were also carried out in a 30-L bioreactor, and the GlcNAc titer and OD_{600} increased by 5.1% and 11% to 124.8 g/L and 108 g/L compared with the strain G-3 (Fig. 4C).

In *E coli*, there is another acetate synthesis pathway besides *poxB*. Phosphate acetyltransferase *pta* genes catalyze the combination of acetyl-CoA and phosphate to generate acetyl phosphate. Then acetate kinase (*ackA*) and acyl phosphatase (*yccX*) convert acetyl phosphate into acetate. Thus, the genes *pta* and *ackA* of strain G-7 were knocked out, yielding G-8 and G-9 strains, respectively. The G-8 strain showed severe

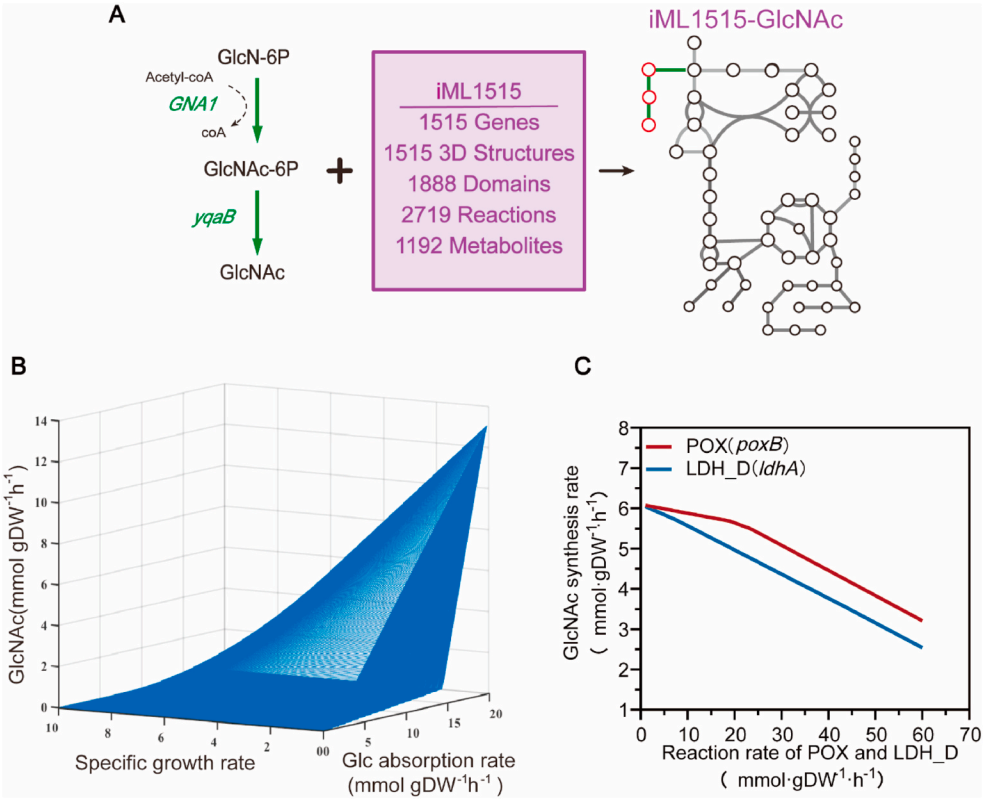

Fig. 3. Construction and application of GSMM. (A) Schematic diagram of metabolic network model construction based on iML1515. (B) Schematic diagram of the relationship between GlcNAc synthesis rate, glucose absorption rate, and specific growth rate. (C) The curve of the specific growth rate of strain G-3 in a 30-L bioreactor fitted by interpolation method. (D) The simulation result of the reaction flux ratio between PFK and *glmS* in the ideal equilibrium state in a 30-L bioreactor.

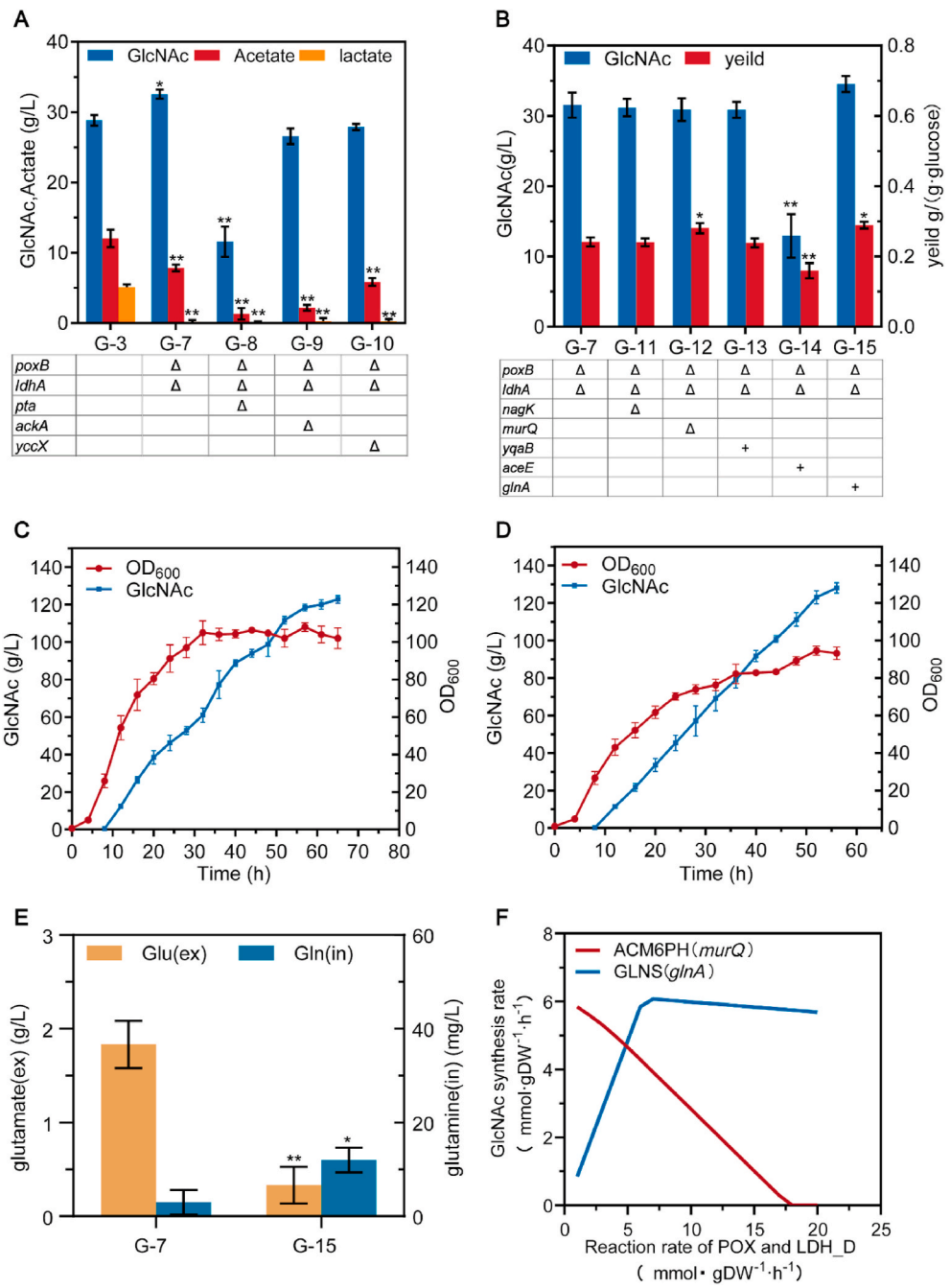

Fig. 4. Effect of blocking competition pathway and enhancing GlcNAc synthesis pathway on production of GlcNAc. (A) Shake flask fermentation results of strains with knockout genes related to acetic acid and lactate synthesis. Δ means knockout. (B) Shake flask fermentation blocks some competition pathway genes and enhances the GlcNAc synthesis pathway. Δ means knockout, + means enhancement. (C) Fermentation result of strain G-7 in 30-L bioreactor. (D) Fermentation result of strain G-16in a 30-L bioreactor. (E) Comparison of extracellular glutamate and intracellular glutamine concentrations during fermentation of strains G-7 and G-15. (F) The effect of the flux change of the *murQ* and *glnA* catalyzed reactions on GlcNAc synthesis in model simulation results. ** and * symbols indicate $p < 0.01$ and $0.01 < p < 0.05$ relative to the control strain, respectively.

growth inhibition, consistent with a previous study that blocked phosphate acetyl synthesis.[18] The shake flask fermentation results showed that both GlcNAc and cell density decreased significantly. This phenomenon did not appear after knocking out the *ackA* gene (G-9 strain), nor did it completely block acetate production. Although acetate production decreased significantly, it did not promote the GlcNAc synthesis. On the contrary, the GlcNAc titer of G-9 strain showed a slight decrease (7.4%). The gene *yccX*, which has similar functions to *ackA*, was knocked out, yielding the strain G-10. The results show that although the *yccX* knockout also reduced the acetate concentration, the GlcNAc production did not increase (Fig. 4A).

There is an N-acetyl-D-glucosamine kinase (*nagK*) in *E. coli*, which catalyzes GlcNAc conversion to GlcNAc-6P.[19] It may form an ineffective cycle with *yqaB*, limiting GlcNAc accumulation and wasting energy. *NagK* gene knocked out yield strain G-11. The *murQ* gene product consumes GlcNAc-6P, the precursor of GlcNAc. It has been reported that knocking out *murQ* promotes GlcN synthesis.[20] The *murQ* gene was knocked out in the G-7 strain, yielding strain G-12. Lee Sang-woo et al. successfully screened *yqaB* phosphatase from *E. coli* and verified its effect on GlcNAc synthesis.[21] Therefore, a P_{T7lac}-*yqaB* cassette was integrated into the G-12 genome, resulting in the G-13 strain. Acetyl-CoA is an acetyl donor for the conversion of GlcN-6P to GlcNAc-6P. To increase the acetyl-CoA supply, a P_{T7lac}-*aceE* cassette was integrated into the genome of strain G-7, resulting in strain G-14. However, *nagK* knockout and *yqaB* integration did not play a significant role, and there was no significant change in titer and yield. The *aceE* gene copy number increase resulted in a 52.6% lower GlcNAc titer (15.7 g/L) in G14 than in strain G-7.

Glutamine is an essential amino donor for the conversion of Fru-6P to GlcN-6P. About 2 g/L glutamate were detected in the fermentation broth

in the bioreactor. Therefore, glutamine synthetase (*glnA*) was overexpressed to enhance the conversion of glutamate to glutamine. One copy of P_{T7lac}-*glnA* was integrated into the G-7 genome (resulting in strain G-15) to verify whether the glutamine supply limited the increase in GlcNAc production. As shown in Fig. 4B, the results of shake flask fermentation showed that the titer and yield of GlcNAc increased in strain G-15, with the titer reaching 35.7 g/L. The enhancement of *glnA* also decreased extracellular glutamate concentration and increased intracellular glutamine concentration (Fig. 4E). Although the G-12 strain did not increase GlcNAc production, it consumed less glucose and produced a titer close to the control group. In the model simulation, the GlcNAc synthesis rate first increased and then decreased with the increase of the GLNS (*glnA*) reaction rate. The ACM6PH (*murQ*) reaction will significantly repress the synthesis of GlcNAc (Fig. 4F). Therefore, we knocked out *murQ* in the G-15 strain to get the G-16 strain. The G-16 strain produced 130.8 g/L of GlcNAc in 56 h in a 30-L bioreactor, a 4.8% increase compared to the G-7 strain. In addition, the GlcNAc yield on glucose reached 44.6% (Fig. 4D).

3.4. Dynamic regulation based on CRISPRi

However, acetate production during the fermentation process was not completely blocked, and the yield was significantly lower than the simulation results. Further analysis of the metabolic flow simulation results showed that the PFK (*pfkAB*) and G6PDH2r (*zwf*) reactions were strictly and dynamically restricted in the optimal simulation results

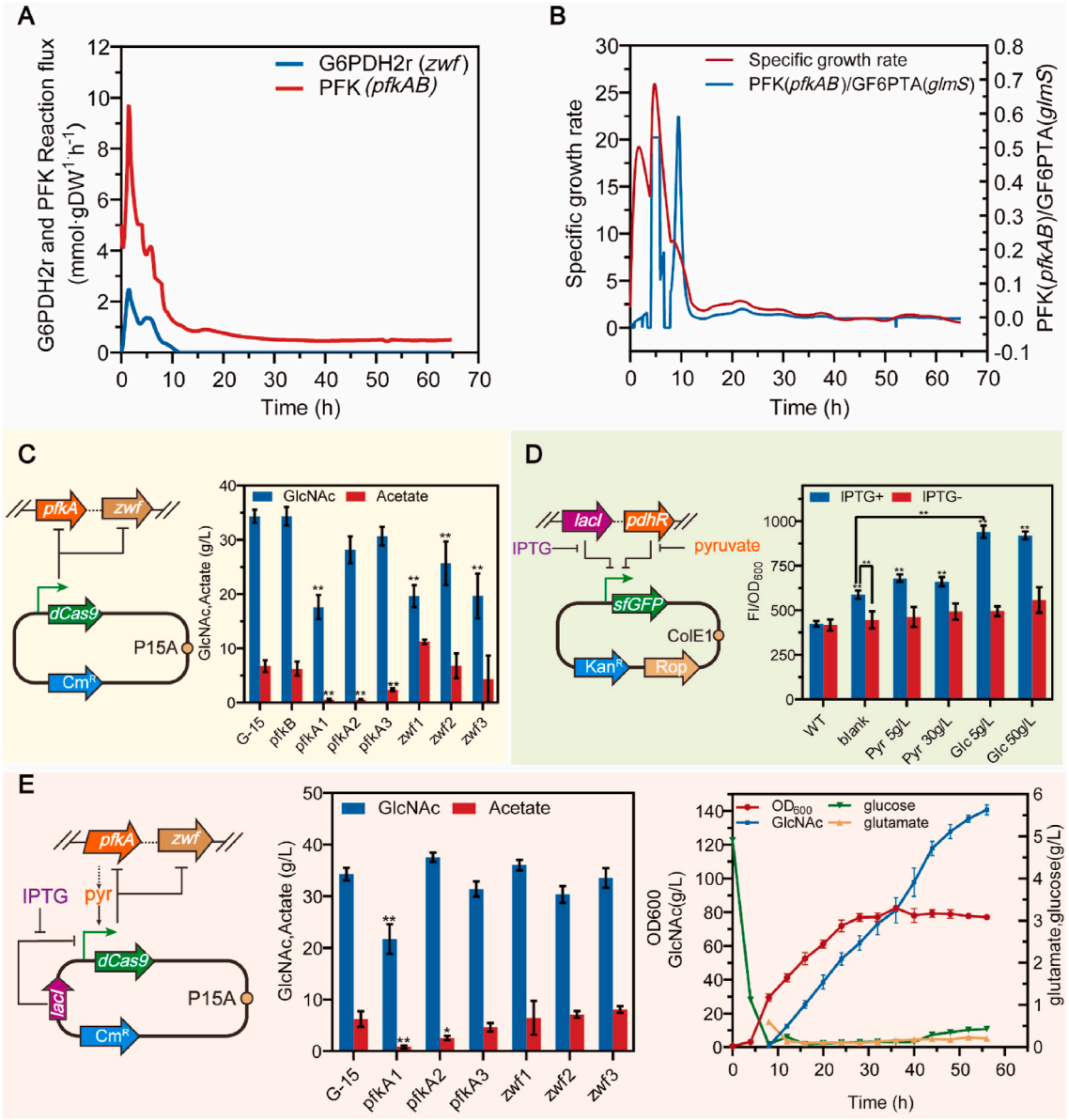

Fig. 5. Construction and application of the dynamic regulatory system. (A) The optimal flux of the reaction catalyzed by *pfkAB* and *zwf* in the simulated fermentation process. (B) Simulated optimal distribution of fluxes catalyzed by *glmS* and *pfkAB*, and specific growth rate during fermentation. (C) Schematic diagram of gene interference with CRISPRi system constitutive expression and results of shake flask fermentation. The dCas9 was under the control of P_{lacUV5}, and one sgRNA was under the control of P_{j23119}. (D) Schematic diagram and fluorescence verification results of the fluorescent reporter gene *sf-GFP* under the control of *lacI* and *pdhR*. The plasmid was transformed into *E. coli JM109*, cultured in a 96-well plate with shaking at 37 °C for 8 h in LB liquid medium to detect the fluorescence intensity of the fermentation broth. Different concentrations of pyruvate and glucose were added with and without IPTG. (E) Schematic diagram and fermentation results of the dynamic regulation on *pfkA* and *zwf* under the control of *pdhR* and *lacI*. ** and * symbols indicate $p < 0.01$ and $0.01 < p < 0.05$ relative to the control strain, respectively.

(Fig. 5A). The flux of the *zwf*-catalyzed reaction remains almost zero after adding the inducer. The reaction catalyzed by *pfkAB* and *glmS* competes for the same substrate, fructose-6-phosphate. The optimal fluxes of the two reactions is always related to the specific growth rate (Fig. 5B).

In *E. coli*, there are two phosphofructokinase isoenzymes, *pfk1* and *pfk2*,encoded by the *pfkA* and *pfkB* genes, respectively. *pfkA* accounts for most enzyme activity.[22] Acetyl-CoA and glutamine are essential acetyl and amino donors for GlcNAc synthesis. *pfkA* gene knockout may result in an insufficient supply of donor materials and severely impact cell growth. The results show that the GlcNAc titer did not show apparent changes after *pfkB* knockout.

It has been reported that the GlcNAc production is increased in *E. coli* and *Bacillus subtilis* by interfering genes *pfkA* and *zwf*.[6,23] Hence, a plasmid was constructed with a CRISPRi system to repress these genes. The CRISPRi system includes a *dCas9* lacking endonuclease activity and a specific guiding sgRNA. When combined with sgRNA, *dCas9* interferes with target genes. The interference intensity of this system has an extensive adjustable range and can interfere with multiple target genes simultaneously.[24,25] Three different target regions of each *pfkA* and *zwf* genes were selected for repression. None of these strains produced more GlcNAc than the control group, as shown by the shake flask fermentation results in Fig. 5C.

To prevent the inhibition of cell growth in seed culture before adding the inducer, a *lacO* was added upstream of the *dCas9* gene. In addition, the pyruvate-responsive transcription regulator *pdhR* was selected to dynamically regulate tdCas9 expression. The *pdhR* transcription regulator in *E. coli* binds to a specific sequence site and inhibits gene expression. When the intracellular pyruvate binds to it, it separates from the binding site releasing the repressive effect.[26] The combination of *pdhR* and CRISPRi system changed the interference intensity with the pyruvate concentration in the cell, which was dynamically adjusted during the fermentation process to maintain the appropriate interference intensity. When the pyruvate concentration is low, the target genes' interference is inhibited. When pyruvate accumulates, CRISPRi inhibitory strength is unlocked, reducing glycolytic flux to prevent by-products production (Fig. 5E).

The dynamic regulation system was verified by the *sf-GFP* reporter to construct the pyruvate response gene circuit. The plasmid pET28a-P_{lacUV5}-*pdhR* box-*lacO-sfGFP* was constructed to verify whether the system was effectively induced by IPTG and its response to pyruvate and glucose. Different pyruvate and glucose concentrations were added into the culture medium to detect changes in the fluorescence intensity of the fermentation broth. Fluorescence intensity shows that this system can respond to pyruvate and glucose, and the fluorescence intensity of the pyruvate group was lower than the glucose group (Fig. 5D). Moreover, *sf-GFP* expression was effectively inhibited in the group without IPTG. To regulate GlcNAc synthesis using this pyruvate response gene circuit, a low copy number plasmid pACYC-P_{lacUV5}-*pdhR* box-*lacO-dCas9-*P_{J23119}-sgRNA was constructed and transformed into strain G-16 after incorporating specific sgRNA. The results show that the *pfkA*2 and *zwf*1 repression increased the GlcNAc titer in the shake flask. The two sgRNAs were combined into a plasmid to simultaneously interfere with *pfkA*2 and *zwf*1 genes. This strain produced 143.8 g/L of GlcNAc in a 30-L bioreactor in 55 h, and the yield reached 0.539 g/g glucose (Fig. 5E).

4. Discussion

There are complex metabolic networks and regulatory mechanisms in microorganisms. Many metabolic pathways and products are not needed for industrialization. The presence of these pathways and products will decrease the yield of the target product and waste raw materials. However, some of these pathways and products are closely related to the growth and reproduction of microorganisms. Therefore, it is required to adopt methods such as blocking, inhibiting, replacing, and selecting appropriate metabolic pathways of target products to maximize materials and energy utilization. The metabolic network model plays an increasingly important role in metabolic engineering.[27,28] The GSMM of *E. coli* is relatively mature and can play a guiding role in pathway design, optimization, and simulation. Therefore, in this work, the GlcNAc synthesis reaction was added to the iML1515 model, and the cobra toolbox was used to analyze and simulate gene knockout and metabolic flow regulation, promoting the increase in titer and yield of GlcNAc.[12]

Enhancing the expression of *glmS* and introducing *GNA1* constructed an efficient GlcNAc synthesis pathway in *E. coli*. Increasing the copy number of these key genes does not affect GlcNAc synthesis, illustrating that the gene expression level is not a restrictive factor to product synthesis. Therefore, we considered enhancing other substrates involved in the reaction. The reaction catalyzed by *glnA* is the main source of amino donors for GlcNAc.[29,30] Therefore, adding a *glnA* copy effectively increases the yield. However, the enhancement of *aceE* and *yqaB* did not result in an effective improvement. These results prove that *aceE* and *yqaB* expression levels can meet the requirements of high GlcNAc production, while overexpression may break the original balance and reduce the yield.

There are many by-product pathways in the generated strains, some of which will lead to the diversion and consumption of carbon sources and nutrients.[17] Pyruvate is an important intermediate in the glycolysis (EMP) pathway. Pyruvate metabolism is also extremely prone to carbon source overflow.[31] The production of organic acids leads to carbon loss, pH changes, and growth inhibition, reducing the yield of target products and causing economic losses. The simulation results show that some approaches are unessential for the cell, so they were blocked. Knockout of the *ldhA* gene significantly decreased lactate concentration in the fermentation broth. Knockout of *poxB* also reduced acetate concentration in the fermentation broth, with limited effects because is not the primary acetate source in the strain. Nevertheless, the knockout of both genes increased the maximum cell density and growth rate that could be achieved and increased the titer of GlcNAc. Other acetate production pathways may play other cell roles, and complete blockade did not further increase production.

The model's simulation results show that balancing the relationship between cell growth and product synthesis is an important method to increase yield.[32] This is also a common challenge in microbial metabolism engineering. PFK is closely related to the growth of bacteria and is also the most important competitive reaction of *glmS*. Only when the PFK reaction rate is limited to an appropriate level can the optimal ratio of bacterial growth and product synthesis be ensured. Thus, the CRISPRi system, an efficient repression tool with a high regulatory range,[22,23] was combined with the pyruvate-responsive transcription factor *pdhR* and the lac operon to interfere with *pfkA* and *zwf*. The GlcNAc titers of different strains in shake flasks are shown in Table 2. In addition, keeping a low glucose concentration during the fermentation process helps reduce acetic acid by-product production. It was challenging to add a feed on the shake flask, while it was easy to detect and add a feed in the bioreactor, so the initial glucose concentration was reduced to 5 g/L. Finally, the GlcNAc titer exceeded 140 g/L in a 30-L bioreactor. The productivity reached 2.61 g/(L·h), and the yield reached 0.539 g/g glucose. In the previous study, a genetically engineered *E. coli* (GLALD-7) could use glycerol and glucose as a mixed carbon source to produce 179 g/L GlcNAc in a 5-L bioreactor within 70 h.[8] GLALD-7 yielded 0.458 g/g total carbon source with a productivity of 2.57 g/L/h.

Overall, the *E. coli* strain engineered in this work has great potential to produce GlcNAc on an industrial scale. Moreover, the method of analyzing genetic engineering strategies through GSMM, which has shown high accuracy here, can guide the construction of other strains. In addition, the dynamic regulation system constructed in this study can be used in other *E. coli* fermentations that use glucose as a carbon source. Although this work provides a case for improving the productivity and economy of microbial GlcNAc synthesis, it is possible to further improve GlcNAc production in *E. coli* by further optimizing the carbon flux.

Table 2
GlcNAc titers of different strains in shake flasks.

Strain	G-0	G-1	G-2	G-3	G-4	G-5	G-7	G-8	G-9	G-10	G-11	G-12	G-13	G-14	G-15	G-17
P_{T7}-*GNA1*	1	1														
P_{T7}-*glmS*	1															
P_{T7}-*glmS**		1														
P_{T7lac}-*GNA1*			1	2	1	2	2	2	2	2	2	2	2	2	2	2
P_{T7lac}-*glmS**			1	1	2	2	1	1	1	1	1	1	1	1	1	1
manXYZ	Δ		Δ	Δ	Δ	Δ	Δ	Δ	Δ	Δ	Δ	Δ	Δ	Δ	Δ	Δ
nagABE	Δ		Δ	Δ	Δ	Δ	Δ	Δ	Δ	Δ	Δ	Δ	Δ	Δ	Δ	Δ
FucIK				Δ	Δ	Δ	Δ	Δ	Δ	Δ	Δ	Δ	Δ	Δ	Δ	Δ
poxB							Δ	Δ	Δ	Δ	Δ	Δ	Δ	Δ	Δ	Δ
LdhA							Δ	Δ	Δ	Δ	Δ	Δ	Δ	Δ	Δ	Δ
pta								Δ								
ackA									Δ							
yccX										Δ						
nagK											Δ					
murQ												Δ				Δ
P_{T7lac}-*yqaB*													1			
P_{T7lac}-*aceE*														1		
P_{T7lac}-*glnA*															1	
pfkA																Repressed
zwf																Repressed
Titer (g/L)	18.7	22.6	25.6	30.7	28.0	29.1	33.2	13.7	27.6	28.4	32.6	32.0	32.1	15.7	35.7	39.8

Authors contribution

J.H.L., G.C.D., and L.L designed the research; J.G.L., and Y.K.W. performed research; J.G.L. analyzed data; Y.K.W., C.D., X.Q.L., Y.F.L., and L.L. wrote and revised the paper. All authors contributed to the manuscript.

Declaration of competing interest

The authors declare that they have no known competing financial interests or personal relationships that could have appeared to influence the work reported in this paper.

Acknowledgments

This work was financially supported by the National Natural Science Foundation of China (31870069 and 32021005), the China National Postdoctoral Program for Innovative Talents (BX2021113), the China Postdoctoral Science Foundation (2021M701458), the Key Research and Development Program of China (2020YFA0908300 and 2018YFA0900300), the Fundamental Research Funds for the Central Universities (USRP52019A, JUSRP121010, and JUSRP221013), and Shandong Province Key R & D Program (Major Science and Technology Innovation Project) Project (2019JZZY011002).

Appendix A. Supplementary data

Supplementary data to this article can be found online at https://doi.org/10.1016/j.biotno.2022.02.001.

References

1 Yadav V, et al. N-acetylglucosamine 6-phosphate deacetylase (nagA) is required for N-acetyl glucosamine assimilation in *Gluconacetobacter xylinus*. *PLoS One*. 2011;6, e18099. https://doi.org/10.1371/journal.pone.0018099.
2 Nakamura H. Application of glucosamine on human disease—Osteoarthritis. *Carbohydr Polym*. 2011;84:835–839. https://doi.org/10.1016/j.carbpol.2010.08.078.
3 Igarashi M, Sakamoto K, Nagaoka I. Effect of glucosamine, a therapeutic agent for osteoarthritis, on osteoblastic cell differentiation. *Int J Mol Med*. 2011;28:373–379. https://doi.org/10.3892/ijmm.2011.686.
4 Deng C, et al. Metabolic engineering of *Corynebacterium glutamicum S9114* based on whole-genome sequencing for efficient N-acetylglucosamine synthesis. *Synth Syst Biotechnol*. 2019;4:120–129. https://doi.org/10.1016/j.synbio.2019.05.002.
5 Deng C, et al. Synergistic improvement of N-acetylglucosamine production by engineering transcription factors and balancing redox cofactors. *Metab Eng*. 2021;67:330–346. https://doi.org/10.1016/j.ymben.2021.07.012.
6 Wu Y, et al. Design of a programmable biosensor-CRISPRi genetic circuits for dynamic and autonomous dual-control of metabolic flux in *Bacillus subtilis*. *Nucleic Acids Res*. 2020;48:996–1009. https://doi.org/10.1093/nar/gkz1123.
7 Deng MD, et al. Metabolic engineering of *Escherichia coli* for industrial production of glucosamine and N-acetylglucosamine. *Metab Eng*. 2005;7:201–214. https://doi.org/10.1016/j.ymben.2005.02.001.
8 Ma Q, et al. Highly efficient production of N-Acetyl-glucosamine in *Escherichia coli* by appropriate catabolic division of labor in the utilization of mixed glycerol/glucose carbon sources. *J Agric Food Chem*. 2021;69:5966–5975. https://doi.org/10.1021/acs.jafc.1c01513.
9 Bernal V, Castano-Cerezo S, Canovas M. Acetate metabolism regulation in *Escherichia coli*: carbon overflow, pathogenicity, and beyond. *Appl Microbiol Biotechnol*. 2016;100:8985–9001. https://doi.org/10.1007/s00253-016-7832-x.
10 Durot M, Bourguignon PY, Schachter V. Genome-scale models of bacterial metabolism: reconstruction and applications. *FEMS Microbiol Rev*. 2009;33:164–190. https://doi.org/10.1111/j.1574-6976.2008.00146.x.
11 Xu P, Ranganathan S, Fowler ZL, Maranas CD, Koffas MA. Genome-scale metabolic network modeling results in minimal interventions that cooperatively force carbon flux towards malonyl-CoA. *Metab Eng*. 2011;13:578–587. https://doi.org/10.1016/j.ymben.2011.06.008.
12 Monk JM, et al. iML1515, a knowledgebase that computes *Escherichia coli* traits. *Nat Biotechnol*. 2017;35:904–908. https://doi.org/10.1038/nbt.3956.
13 Deng MD, et al. Directed evolution and characterization of *Escherichia coli* glucosamine synthase. *Biochimie*. 2006;88:419–429. https://doi.org/10.1016/j.biochi.2005.10.002.
14 Datsenko KA, Wanner BL. One-step inactivation of chromosomal genes in *Escherichia coli K-12* using PCR products. *Proc Natl Acad Sci U S A*. 2000;97:6640–6645. https://doi.org/10.1073/pnas.120163297.
15 Heirendt L, et al. Creation and analysis of biochemical constraint-based models using the COBRA Toolbox v.3.0. *Nat Protoc*. 2019;14:639–702. https://doi.org/10.1038/s41596-018-0098-2.
16 Mahadevan R, Schilling CH. The effects of alternate optimal solutions in constraint-based genome-scale metabolic models. *Metab Eng*. 2003;5:264–276. https://doi.org/10.1016/j.ymben.2003.09.002.
17 Causey TB, Shanmugam KT, Yomano LP, Ingram LO. Engineering *Escherichia coli* for efficient conversion of glucose to pyruvate. *Proc Natl Acad Sci U S A*. 2004;101:2235–2240. https://doi.org/10.1073/pnas.0308171100.
18 Lozano Terol G, Gallego-Jara J, Sola Martinez RA, Canovas Diaz M, de Diego Puente T. Engineering protein production by rationally choosing a carbon and nitrogen source using *E. coli BL21* acetate metabolism knockout strains. *Microb Cell Factories*. 2019;18:151. https://doi.org/10.1186/s12934-019-1202-1.
19 Neitzel LR, et al. Developmental regulation of Wnt signaling by *Nagk* and the UDP-GlcNAc salvage pathway. *Mech Dev*. 2019;156:20–31. https://doi.org/10.1016/j.mod.2019.03.002.
20 Li P, et al. Enhancement of production of D-glucosamine in *Escherichia coli* by blocking three pathways involved in the consumption of GlcN and GlcNAc. *Mol Biotechnol*. 2020;62:387–399. https://doi.org/10.1007/s12033-020-00257-9.
21 Lee SW, Oh MK. A synthetic suicide riboswitch for the high-throughput screening of metabolite production in Saccharomyces cerevisiae. *Metab Eng*. 2015;28:143–150. https://doi.org/10.1016/j.ymben.2015.01.004.
22 Siedler S, Bringer S, Bott M. Increased NADPH availability in *Escherichia coli*: improvement of the product per glucose ratio in reductive whole-cell biotransformation. *Appl Microbiol Biotechnol*. 2011;92:929–937. https://doi.org/10.1007/s00253-011-3374-4.
23 Zhang Q, et al. CRISPRi-based dynamic control of carbon flow for efficient N-acetyl glucosamine production and its metabolomic effects in *Escherichia coli*. *J Agric Food Chem*. 2020;68:3203–3213. https://doi.org/10.1021/acs.jafc.9b07896.

24 Qi LS, et al. Repurposing CRISPR as an RNA-guided platform for sequence-specific control of gene expression. *Cell*. 2013;152:1173–1183. https://doi.org/10.1016/j.cell.2013.02.022.
25 Zalatan JG, et al. Engineering complex synthetic transcriptional programs with CRISPR RNA scaffolds. *Cell*. 2015;160:339–350. https://doi.org/10.1016/j.cell.2014.11.052.
26 Anzai T, Imamura S, Ishihama A, Shimada T. Expanded roles of pyruvate-sensing PdhR in transcription regulation of the *Escherichia coli K-12* genome: fatty acid catabolism and cell motility. *Microb Genom*. 2020;6. https://doi.org/10.1099/mgen.0.000442.
27 Rau MH, Zeidan AA. Constraint-based modeling in microbial food biotechnology. *Biochem Soc Trans*. 2018;46:249–260. doi:10.1042/BST20170268.
28 Schopping, M., Gaspar, P., Neves, A. R., Franzen, C. J. & Zeidan, A. A. Identifying the essential nutritional requirements of the probiotic bacteria *Bifidobacterium* animalis and *Bifidobacterium longum* through genome-scale modeling. NPJ Syst Biol Appl 7, 47, doi:10.1038/s41540-021-00207-4 (2021).
29 Isupov MN, et al. Substrate binding is required for assembly of the active conformation of the catalytic site in Ntn amidotransferases: evidence from the 1.8 A crystal structure of the glutaminase domain of glucosamine 6-phosphate synthase. *Structure*. 1996;4:801–810. https://doi.org/10.1016/s0969-2126(96)00087-1.
30 Pearson JT, Dabrowski MJ, Kung I, Atkins WM. The central loop of *Escherichia coli* glutamine synthetase is flexible and functionally passive. *Arch Biochem Biophys*. 2005;436:397–405. https://doi.org/10.1016/j.abb.2005.02.008.
31 De Anda R, et al. Replacement of the glucose phosphotransferase transport system by galactose permease reduces acetate accumulation and improves process performance of *Escherichia coli* for recombinant protein production without impairment of growth rate. *Metab Eng*. 2006;8:281–290. https://doi.org/10.1016/j.ymben.2006.01.002.
32 Pandit AV, Srinivasan S, Mahadevan R. Redesigning metabolism based on orthogonality principles. *Nat Commun*. 2017;8:15188. https://doi.org/10.1038/ncomms15188.
33 Jiang Y, et al. Multigene editing in the *Escherichia coli* genome via the CRISPR-Cas9 system. *Appl Environ Microbiol*. 2015;81:2506–2514. https://doi.org/10.1128/AEM.04023-14.